Fermi National Accelerator Laboratory

FERMILAB-Pub-88/67-A
May 1988

STABILITY OF BOSON STARS

Marcelo Gleiser [†]

NASA/Fermilab Astrophysics Center
MS209 Fermi National Accelerator Laboratory
Box 500, Batavia, IL 60510

ABSTRACT

Boson stars are gravitationally bound, spherically symmetric equilibrium configurations of cold, free or interacting complex scalar fields ϕ. As these equilibrium configurations naturally present local anisotropy, it is sensible to expect departures from the well known stability criteria for fluid stars. With this in mind, I investigate the dynamical instability of boson stars against charge conserving, small radial perturbations. Following the method developed by Chandrasekhar, a variational base for determining the eigenfrequencies of the perturbations is found. This approach allows one to find numerically an *upper bound* for the central density where dynamical instability occurs. As applications of the formalism, I study the stability of equilibrium configurations obtained both for the free and for the self-interacting (with $V(\phi) = \frac{\lambda}{4}|\phi|^4$) massive scalar field ϕ. Instabilities are found to occur not for the critical central density as in fluid stars but for central densities considerably higher. The departure from the results for fluid stars is sensitive to the coupling λ; the higher the value of λ, the more the stability properties of boson stars approach those of a fluid star. These results are linked to the fractional anisotropy at the radius of the configuration.

[†] Address after September 1988: Institute for Theoretical Physics, University of California at Santa Barbara, Santa Barbara, CA 93106.

1. Introduction

In recent years, the active interplay between particle physics and cosmology has made frequent use of scalar fields as driving the dynamics and the formation of structure in the early Universe. This current interest in the possible role scalar fields may have played in primordial phase transitions or as sources of dark-matter, has raised interesting questions as to whether cold, spherically symmetric and stable configurations of complex scalar fields, "boson stars", could exist in which the gravitational contribution to the total energy of the configurations can not be neglected.

Boson stars are to be contrasted with other localized, stable, scalar field configurations that have been proposed in the literature in which gravity does not play a role, such as non-topological solitons and Q-balls [1]. These objects owe their stability (against dispersion of the scalar particles to infinity) to the balance between two opposing terms in the expression for their energy: Non-trivial couplings in the effective potential generate surface and/or volume terms that act to localize the field configuration. The effective pressure that balances this effect is actually common to both boson stars and non-topological solitons. It comes from the conservation of charge associated with a global symmetry of the model. For a global $U(1)$, this charge is related to the number of particles (minus anti-particles) in the configuration, N (although, of course, any additive quantum number will do). Thus, if N is bigger than a calculable minimum value, the particles will resist localization with an effective pressure that scales with $\sim 1/R$, where R is the typical size of the configuration. The bigger the charge the more bound is the object. The importance of gravity also grows with the charge. One may think of soliton stars or Q-stars where the charge of the non-topological soliton is big enough to justify gravitational corrections to the energy. Although these objects are very interesting (more about them later), as a first step I will forget about the non-trivial couplings and consider only free or self-interacting (with quartic coupling) scalar fields. This takes us back to the realm of boson stars.

The first step in understanding boson stars was taken by Ruffini and Bonazzola [2]. They have found interior Schwarzschild solutions to the Einstein-Klein-Gordon system with the simplifying assumptions that the scalar field is nodeless and at zero temperature, i.e., that the field forms a condensate with zero-momentum $p \sim 1/R \sim m$, where m is the scalar field mass and R is the typical size of the configuration. Thus, the equilibrium configurations can be thought of as being macroscopic quantum states of cold, degenerate bosons held together by gravity with supporting pressure given by Heisenberg's uncertainty principle. The results in [2] have been recently confirmed by the works listed in [3].

In [2] it was shown that, although boson stars have many similarities to their fermionic counterparts, white dwarfs and neutron stars, there are also many interesting differences, that call for a detailed study of these objects. As a first example, boson stars also exhibit a critical mass and critical particle number, given respectively by $M_{crit} = 0.633 M_{Planck}^2/m$ and $N_{crit} = 0.653 M_{Planck}^2/m^2$, where M_{Planck} is the Planck mass. The order of magnitude estimates for M_{crit} and N_{crit} can be easily obtained using Landau's argument adapted for a bosonic configuration; just minimize the energy of a scalar particle with the above momentum in the background gravitational potential of all self-gravitating particles, $E_p \sim -GMm/R$. Note, however, that the Chandrasekhar mass is $M_{Chan} \sim M_{Planck}^3/m^2$, while the critical particle number goes as $N_{Chan} \sim M_{Planck}^3/m^3$. Thus, for fields of mass $\sim$

1Gev we obtain boson stars of mass $\sim 10^{17}$g and 10^{38} particles, much lighter than their fermionic counterparts which would, instead, have a mass $\sim 10^{33}$g with $\sim 10^{57}$ particles. It is also worth mentioning that the critical density for boson stars is $\rho_{crit}(0) = 8.3 \times 10^{52}(\frac{m}{Gev})$gcm^{-3}, enormously higher than that for cold, degenerate fermions! Densities of this order are found for objects with sizes comparable to the Compton wavelength of their constituent particles. Clearly, at such densities we may expect deviations from the common lore concerning stability of fluid stars.

A parenthesis should be opened here concerning higher node solutions. As mentioned before, the above critical values are all related to nodeless field configurations. In the work by Friedberg, Lee and Pang [3] it was shown that if one considers only the spherically symmetric higher nodes (i.e., with ℓ, the angular momentum quantum number being zero), the critical mass grows approximately linearly for large node number $n-1$. The same tendency was observed for scalar fields with non-minimal coupling in the work by van der Bij and Gleiser [4]. If a given configuration happens to contain too many particles to be a zero node equilibrium configuration, it would possibly find equilibrium in a configuration with the number of nodes necessary to accomodate the total number of particles. Nevertheless, despite the difference in node number, the equilibrium configurations obtained all have very similar properties. In particular, what is crucial to the stability analysis is that they all share the existence of a critical mass. In this work I will look only into the simplest zero node configurations. The stability analysis to be developed here can be extended to higher spherical nodes without too much problem. The results should be qualitatively similar.

Boson stars with self-interacting scalar fields have been considered in the work by Colpi, Shapiro and Wasserman [5]. One of the consequences of switching on a repulsive self-interaction between the scalar particles is to increase the above critical limits on the mass and particle number. In particular, if $m_{boson} \equiv \lambda^{1/4} m_{fermion}$, the critical mass for the boson star approaches the Chandrasekhar limit. Other models, including soliton stars [6] and boson stars with non-minimal coupling for the scalar field [4], have confirmed the same tendency; interactions tend to increase the critical values for mass and particle number, although the particular values are very model dependent. An extreme example is obtained for soliton stars, where the critical mass scales as $M_{crit} \sim M_{Pl}^4/m^3$.

One of the crucial differences between the bosonic and the fermionic configurations arises if one tries to implement a macroscopic description for the bosonic condensate †. As it was already shown in [2] and later emphasized in more recent work [3], it is not consistent with the field equations to describe the bosonic condensate as a perfect fluid with a given equation of state; the energy-momentum tensor is not isotropic in the 3 spatial directions, with the radial component differing from the 2 angular components. Due to this local anisotropy, the most general form of the energy-momentum tensor is $T^\mu_\nu = diag(\rho, -p_r, -p_\perp, -p_\perp)$, where p_r is the radial pressure and $p_\perp$ is the tangential pressure. As an immediate consequence, we can not apply directly the well known theorems for

† By fermionic configurations I mean configurations with supporting pressure given by Pauli's exclusion principle, such as white dwarfs and neutron stars. These should be distinguished from fermion soliton stars [6] that exist due to a non-trivial coupling between the fermions and a real scalar field.

stellar stability when dealing with boson stars. Nevertheless, if we plot mass against central density for these stars, we will find a behaviour remarkably similar to those of neutron stars: In the plot of total mass against central density, the mass M quickly raises to a maximum (at $\sigma(0) = \sigma_{crit}(0) = 0.271$, where $\sigma(0)$ is the dimensionless value of the scalar field at the origin which is used as a parametrization of the central density of the configuration), drops a little, oscillates and approaches an asymptotic value at large central densities, the same happening for the particle number N (see fig. 1). Note also that the binding energy $E_b \equiv M - Nm$ becomes positive for a finite value of the central density (at $\sigma_{crs}(0) = 0.54$), suggesting the existence of configurations with excess energy (or fissionable). Such configurations are unstable in principle against a collective transformation in which they are dispersed into free particles at infinity. The excess energy is translated into kinetic energy of the free particles. Nevertheless, they are (as any equilibrium configuration is) stable against removal of individual particles; at the surface of the configuration, the mass-energy necessary to create a particle is $m(1 - 2M/R)^{1/2}$, which is less than the energy needed to create a scalar particle at infinity. Also, as shown by Zel'dovich and Novikov [7], there may be equilibrium configurations with excess energy which are stable against small radial perturbations.

At first sight, the existence of a critical mass suggests that for $M > M_{crit}$ gravitational collapse will be unavoidable. For boson stars things are not so simple, since, as was stressed before, it is possible that such heavy configurations will reach equilibrium with $n - 1 > 0$†. But this is not the only way collapse can occur. From the theory of stellar stability we know that equilibrium configurations with central densities $\rho(0) > \rho_{crit}(0)$ are unstable to small radial perturbations [7]. Most of the previous papers on boson stars have conjectured that similar results would be found once a microscopic approach to the stability analysis was known.

In this paper I address the question of the stability of bosonic equilibrium configurations against radial oscillations both for the free and for the self-interacting case, with $V(\phi) = \frac{\lambda}{4}|\phi|^4$. In fact, the present formalism can be extended to any interacting potential for the scalar field. (The extension to soliton stars [6] is more subtle). I will adapt Chandrasekhar's formalism for studying dynamical instability of fluid stars against small radial oscillations [8] to scalar fields with a given energy-momentum tensor. A variational approach is used to obtain an upper bound for the eigenfrequencies of the perturbations for different values of the central density and given trial functions. As will be shown, the existence of pressure anisotropy has a big impact on the stability properties of boson stars; contrary to the results for fluid stars, instabilities are found not for central densities equal or larger than the critical density but for configurations well to the right of the maximum mass (see figures 1 and 2).

The paper is organized as follows; in section 2 the basic formalism to obtain the equilibrium configurations for boson stars with the potential $V(\phi) = \frac{\lambda}{4}|\phi|^4$ for the scalar field is developed. In section 3 some interesting properties of the equilibrium configurations not previously discussed in the literature are presented. In particular, for a given value of

† As shown in Friedberg, Lee and Pang [3] high node configurations are unstable against fission. The mass can not grow indefinitely.

λ, the fractional anisotropy at the radius of the stellar configuration $fa = (p_r - p_\perp)/p_r$ shows a very regular pattern that is roughly independent of the central density and plays a crucial role in the understanding of the stability results later on. In section 4, I extend the formalism to first order radial perturbations and obtain the linearized dynamical equations that govern their evolution. It is shown that the problem can be reduced to two coupled eigenvalue equations for the two real components of the perturbations of the scalar field, and how a variational base that is used to give an upper bound to the eigenfrequencies of the perturbations can be built. It is also shown how the formalism is compatible with charge-conserving perturbations. The formalism of section 4 can then be used, with suitable trial functions for the perturbations, to numerically obtain *upper bounds* for their eigenfrequencies for different values of the central density. This is done in section 5 both for the free case and for the self-interacting case. The relation between the results found and the fractional anisotropy introduced in section 3 is stressed.

I conclude in section 6 with a summary of the results and with an outlook to future work.

2. Equilibrium Configurations

The starting point for the calculation is the action

$$S = \int d^4x\sqrt{-g}\left[\frac{R}{16\pi G} + g^{\mu\nu}\phi^*_{;\mu}\phi_{;\nu} - m^2|\phi|^2 - \frac{\lambda}{4}|\phi|^4\right]. \tag{1}$$

This action is invariant under a global phase transformation, $\phi \to e^{i\theta}\phi$, that implies the conservation of its generator N, the total particle number. By varying the action with respect to $g^{\mu\nu}$ and ϕ (or equivalently ϕ^*), we obtain respectively Einstein equations

$$R_{\mu\nu} - \frac{1}{2}g_{\mu\nu}R = -8\pi G T_{\mu\nu} \quad , \tag{2}$$

with

$$T_{\mu\nu} = \phi^*_{,\mu}\phi_{,\nu} + \phi^*_{,\nu}\phi_{,\mu} - g_{\mu\nu}\left[g^{\alpha\beta}\phi^*_{,\alpha}\phi_{,\beta} - m^2|\phi|^2 - \frac{\lambda}{4}|\phi|^4\right] \tag{3}$$

and the scalar field equation

$$g^{\alpha\beta}\phi_{;\alpha\beta} + m^2\phi + \frac{\lambda}{2}|\phi|^2\phi = 0. \tag{4}$$

As we are considering a spherically symmetric system with motions only in the radial direction, we take as the spacetime metric

$$ds^2 = e^\nu dt^2 - e^\lambda dr^2 - r^2(d\theta^2 + sin^2\theta d\varphi^2) \quad , \tag{5}$$

where ν and λ are functions of r and t only. The distinction between the metric function λ and the coupling constant with same notation should be obvious throughout the text. It is also convenient to write the scalar field as

$$\phi(r,t) = [\phi_1(r,t) + i\phi_2(r,t)]e^{-i\omega t} \quad , \tag{6}$$

where $\phi_1(r,t)$ and $\phi_2(r,t)$ are real functions. With the metric (5) Einstein equations are

$$R_0^0 - \frac{1}{2}R = -8\pi G T_0^0 \equiv -8\pi G\rho = \frac{1}{r^2}(re^{-\lambda})' - \frac{1}{r^2} \tag{7}$$

$$R_1^1 - \frac{1}{2}R = -8\pi G T_1^1 \equiv 8\pi G p_r = e^{-\lambda}(\frac{\nu'}{r} + \frac{1}{r^2}) - \frac{1}{r^2} \tag{8}$$

$$\begin{aligned} R_2^2 - \frac{1}{2}R = R_3^3 - \frac{1}{2}R = -8\pi G T_2^2 = -8\pi G T_3^3 \equiv 8\pi G p_\perp = \\ e^{-\lambda}\left[\frac{1}{2}\nu'' - \frac{1}{4}\nu'\lambda' + \frac{1}{4}\nu'^2 + \frac{1}{2r}(\nu' - \lambda')\right] \\ - e^{-\nu}\left[-\frac{1}{4}\dot{\lambda}\dot{\nu} + \frac{1}{2}\ddot{\lambda} + \frac{1}{4}(\dot{\lambda})^2\right] \end{aligned} \tag{9}$$

and

$$R_0^1 = -8\pi G T_0^1 = \frac{e^{-\lambda}}{r}\dot{\lambda} \quad , \tag{10}$$

where the prime and the dot denote differentiation with respect to r and t respectively. For future convenience, the energy density ρ, the radial pressure p_r, and the tangential pressure $p_\perp$ were introduced. Combining (7) and (8) we obtain the useful relation

$$\frac{e^{-\lambda}}{r}(\lambda' + \nu') = -8\pi G(T_1^1 - T_0^0) \quad . \tag{11}$$

As it is well known, equations (7)-(10) are not all independent due to the Bianchi identities. As a consequence, the conservation of energy-momentum $T^\nu_{\mu;\nu} = 0$ leads, in the present framework, to

$$\dot{T}_0^0 + T_0^{1\prime} + \frac{1}{2}(T_0^0 - T_1^1)\dot{\lambda} + T_0^1\left[\frac{1}{2}(\lambda' + \nu') + \frac{2}{r}\right] = 0 \tag{12}$$

and

$$\dot{T}_1^0 + T_1^{1\prime} + \frac{1}{2}T_1^0(\dot{\lambda} + \dot{\nu}) + \frac{1}{2}(T_1^1 - T_0^0)\nu' + \frac{2}{r}(T_1^1 - T_2^2) = 0 \quad . \tag{13}$$

The equations for ϕ_1 and ϕ_2 can be obtained by using (5) and (6) into equation (4) and its complex conjugate giving,

$$\begin{aligned} &\phi_1'' + (\frac{2}{r} + \frac{\nu'}{2} - \frac{\lambda'}{2})\phi_1' + e^{\lambda}(\omega^2 e^{-\nu} - m^2 - \frac{\lambda}{2}\phi_1^2)\phi_1 \\ &- e^{\lambda-\nu}\ddot{\phi}_1 + \frac{1}{2}e^{\lambda-\nu}(\dot{\nu} - \dot{\lambda})\dot{\phi}_1 \pm \frac{1}{2}e^{\lambda-\nu}(\dot{\nu} - \dot{\lambda})\omega\phi_2 \\ &\mp 2e^{\lambda-\nu}\omega\dot{\phi}_2 - e^{\lambda}(\frac{\lambda}{2})\phi_1\phi_2^2 = 0 \quad , \end{aligned} \tag{14}$$

where the equation for ϕ_2 is obtained by interchanging the subscripts $1 \leftrightarrow 2$ and by taking the lower signs.

Finally, as mentioned before, the global invariance of the action (1) leads to the continuity equation,

$$J^{\mu}_{;\mu} = 0 \quad , \tag{15}$$

where the current four-vector J^{μ} is given by

$$J^{\mu} = ig^{\mu\nu}(\phi_{,\nu}\phi^{*} - \phi^{*}_{,\nu}\phi) \quad . \tag{16}$$

The conserved charge is then

$$N = \int d^3x \sqrt{-g} J^0 \quad . \tag{17}$$

For the equilibrium configurations the metric functions are time independent. Also, the scalar field components can be written as $\phi_1(r,t) = \phi_0(r)$ and $\phi_2(r,t) = 0$. Thus, there are only three unknown functions of r to be determined; ν_0, λ_0 and ϕ_0, where the subscript 0 is used to characterize the equilibrium quantities. There must be only three independent equations. First note that for the static solutions, equations (10), (12) and (15) are trivially satisfied. Also, equation (13) (the hydrostatic equilibrium equation) is identical to (14) which can be obtained from a combination of equations (7)-(9). It is then a matter of choice which set of equations is taken to be independent; one can use Einstein equations (7)-(9) or, say, equations (7), (8) and (13). I will follow the current practice [2-5] and take the latter combination. The reason I am stressing this point now is that, when we analyse the equations for the perturbations in section 4, matters will not be so simple. We are left with the three equations

$$(re^{-\lambda_0})' = 1 - 8\pi G r^2 \left[(m^2 + \frac{\lambda}{4}\phi_0^2 + e^{-\nu_0}\omega^2)\phi_0^2 + e^{-\lambda_0}\phi_0'^2\right] \tag{18}$$

$$\frac{e^{-\lambda_0}}{r}\nu_0' - \frac{1}{r^2}(1 - e^{-\lambda_0}) = -8\pi G\left[(m^2 - e^{-\nu_0}\omega^2 + \frac{\lambda}{4}\phi_0^2)\phi_0^2 - e^{-\lambda_0}\phi_0'^2\right] \tag{19}$$

$$\phi_0'' + \left(\frac{2}{r} + \frac{\nu_0' - \lambda_0'}{2}\right)\phi_0' - e^{\lambda_0}(m^2 - e^{-\nu_0}\omega^2 + \frac{\lambda}{2}\phi_0^2)\phi_0 = 0 \quad . \tag{20}$$

Equation (11) becomes,

$$\lambda_0' + \nu_0' = 16\pi G r(e^{\lambda_0 - \nu_0}\omega^2\phi_0^2 + \phi_0'^2) \quad . \tag{21}$$

These equations can be integrated numerically once we introduce the dimensionless variables $x \equiv rm, \sigma(r) \equiv (8\pi G)^{1/2}\phi_0(r)$, with the factor ω^2/m^2 being absorbed into the definition of the metric function e^{ν_0}. Note that the coupling λ is replaced by $\Lambda \equiv \frac{\lambda M^2_{Planck}}{8\pi m^2}$. The boundary conditions are $\lambda_0(r=0) = 0, \sigma(r=0) = \sigma(0), \sigma'(r=0) = 0$ and $\sigma(\infty) = 0$. For details see references [2-5]. In figures 1 and 2 we plot the total mass M and particle number N against $\sigma(0)$ for the equilibrium configurations obtained by taking $\Lambda = 0$ and $\Lambda = 60$ respectively. The total mass M is defined by,

$$M = 4\pi\int_0^{\infty} \rho r^2 dr \quad . \tag{22}$$

Note the existence of a critical mass and particle number and how the extrema of the two curves overlap. Note also that, as already mentioned in the introduction, for a finite value of the central density, the binding energy of the configurations $E_b \equiv M - Nm$ becomes positive, signaling the existence of configurations with excess energy. Of course, for $\Lambda > 0$ the repulsive meson-meson interaction not only increases the number of particles in a configuration of given central density but also makes the binding more difficult, explaining why configurations with excess energy occur for smaller values of $\sigma(0)$. As shown in [4], an attractive coupling, if large enough, may make E_b negative definite.

3. Some Properties of the Equilibrium Configurations

In this section I will look in more detail into the equilibrium configurations. In equations (7)-(9) the energy density and the radial and tangential pressures were introduced. For a fluid star, at least up to nuclear densities, there is no reason to include local anisotropy in the equation of state. Nevertheless, there has been some interest in the past in the possible consequences of local anisotropy to properties of compact objects such as surface redshift and critical mass [9]. It has been shown that anisotropy is responsible for changes in these properties and that these changes can be related to the fractional anisotropy ($= fa$) defined by

$$fa \equiv (p_r - p_\perp)/p_r \quad . \tag{23}$$

Clearly, fa measures the departure from local isotropy. To the best of my knowledge, the importance of anisotropy has not been much explored ever since, the main reason being the apparent lack of any realistic object that would naturally display it. Leaving the question of reality aside for the moment, boson stars are ideal subjects for an extensive analysis of the effects of anisotropy [10]. Using the definitions of p_r and $p_\perp$ in equations (8) and (9) combined with the expression for the energy-momentum for the equilibrium configurations, the fractional anisotropy is

$$fa = \frac{2\phi_0'^2}{(e^{-\nu_0}\omega^2 - m^2 - \frac{\lambda}{4}\phi_0^2)\phi_0^2 + e^{-\lambda_0}\phi_0'^2} \quad . \tag{24}$$

In figures 3 and 4, the fractional anisotropy is shown for $\Lambda = 0$ and $\Lambda = 60$ respectively, for different values of the central density. The dots correspond to the values of fa at the radius of the configuration, where the radius is defined as

$$R \equiv \frac{4\pi}{M} \int_0^\infty \rho r^3 dr \quad . \tag{25}$$

Other definitions for the radius, although not as natural as the one above, have been used in the literature [3,4]. The present results are qualitatively the same, independently of the definition used for the radius. There are two important features to be noted. First, for a given Λ, the fractional anisotropy at the radius (FAR) lies very much *on a straight line*, with deviations, for $\Lambda = 0$, of only a few percent. For larger values of Λ the fit is still good, although there are deviations of up to 30% for the smaller and bigger values of the central density as can be seen in table 1. Second, and this is important to the stability analysis, *the higher the value of Λ the smaller is the FAR*. Thus, we should expect that configurations with large enough values of Λ have stability properties similar to those of fluid stars. In reference [5] it has been shown that in the limit $\Lambda \to \infty$ it is possible to write an effective isotropic equation of state for the bosonic matter so that the well known theorems for stability can be successfully applied. Using the present approach, we will see that it is possible to map the deviations from the fluid star results to the FAR. Another interesting property of the equilibrium configurations is shown in table 2; if we write $\sigma_{crit}(0)$ for the central density at the maximum and $\sigma_{crs}(0)$ for the central density at the point where $E_b = 0$, we find that, *independently of* Λ, $\sigma_{crs}(0)/\sigma_{crit}(0) \simeq 2$.

4. Radial Perturbations and Variational Principle

Consider that the equilibrium configurations described in the last two sections are perturbed in such a way that spherical symmetry is maintained. These perturbations will give rise to motions in the radial direction. The equations for the perturbations will be obtained by considering only their first order contributions, i.e., by neglecting all terms of second or higher order in the perturbed quantities. We can thus write

$$\lambda = \lambda_0 + \delta\lambda,\ \nu = \nu_0 + \delta\nu,\ \phi_1 = \phi_0(1 + \delta\phi_1),\ \phi_2 = \phi_0 \delta\dot{\phi}_2 \tag{26}$$

for the various perturbed quantities. The definition of $\delta\phi_2$ with the time derivative will prove to be extremely useful later on, in connection with charge conservation.

In first order, equations (7)-(10) become respectively

$$(re^{-\lambda_0}\delta\lambda)' = 8\pi G r^2 \delta T_0^0 \quad , \tag{27}$$

with

$$\begin{aligned}\delta T_0^0 = \delta\rho = & -\delta\nu\omega^2\phi_0^2 e^{-\nu_0} - \delta\lambda\phi_0'^2 e^{-\lambda_0} + 2e^{-\nu_0}\omega^2\phi_0^2\delta\phi_1 - 2e^{-\nu_0}\omega\phi_0^2\delta\ddot{\phi}_2 \\ & + 2e^{-\lambda_0}\phi_0'^2\delta\phi_1 + 2e^{-\lambda_0}\phi_0\phi_0'\delta\phi_1' + 2m^2\phi_0^2\delta\phi_1 + \lambda\phi_0^4\delta\phi_1 \quad ,\end{aligned} \tag{28}$$

$$\frac{1}{r}(\delta\nu' - \nu_0'\delta\lambda)e^{-\lambda_0} = \frac{e^{-\lambda_0}}{r^2}\delta\lambda - 8\pi G\delta T_1^1 \quad , \tag{29}$$

with

$$\delta T_1^1 = -\delta p_r = -\delta T_0^0 + (4m^2 + 2\lambda\phi_0^2)\phi_0^2\delta\phi_1 \quad , \tag{30}$$

$$\begin{aligned}& e^{-\lambda_0}[\frac{1}{2}\delta\nu'' - \frac{1}{4}\nu_0'\delta\lambda' - \frac{1}{4}\lambda_0'\delta\nu' + \frac{1}{2}\nu_0'\delta\nu' + \frac{1}{2r}(\delta\nu' - \delta\lambda')] - \frac{1}{2}e^{-\nu_0}\ddot{\delta\lambda} \\ & - \delta\lambda[\frac{1}{2}\nu_0'' - \frac{1}{4}\nu_0'\lambda_0' + \frac{1}{4}\nu_0'^2 + \frac{1}{2r}(\nu_0' - \lambda_0')] = -8\pi G\delta T_2^2\end{aligned} \tag{31}$$

with

$$\begin{aligned}\delta T_2^2 = & -\delta p_\perp = \delta\nu\omega^2\phi_0^2 e^{-\nu_0} - \delta\lambda e^{-\lambda_0}\phi_0'^2 - 2e^{-\nu_0}\omega^2\phi_0^2\delta\phi_1 + 2e^{-\nu_0}\omega\phi_0^2\delta\ddot{\phi}_2 \\ & + 2e^{-\lambda_0}\phi_0'^2\delta\phi_1 + 2e^{-\lambda_0}\phi_0\phi_0'\delta\phi_1' + 2m^2\phi_0^2\delta\phi_1 + \lambda\phi_0^4\delta\phi_1\end{aligned} \tag{32}$$

and, finally,

$$\dot{\delta\lambda} = 16\pi G r\phi_0[\phi_0'\delta\dot{\phi}_1 - \omega\phi_0\delta\dot{\phi}_2'] \quad . \tag{33}$$

The equation for $\delta\phi_1$ can be obtained by inserting the perturbations either in equation (13) or (14) since these are identical. We obtain

$$\delta\phi_1'' + \left(\frac{2}{r} + \frac{\nu_0' - \lambda_0'}{2} + 2\frac{\phi_0'}{\phi_0}\right)\delta\phi_1' + \frac{1}{2}\frac{\phi_0'}{\phi_0}(\delta\nu' - \delta\lambda') - e^{\lambda_0 - \nu_0}(2\omega\delta\ddot{\phi}_2 + \delta\ddot{\phi}_1)$$
$$+ e^{\lambda_0-\nu_0}\omega^2(\delta\lambda - \delta\nu) - e^{\lambda_0}\lambda\phi_0^2\delta\phi_1 - e^{\lambda_0}(m^2 + \frac{\lambda}{2}\phi_0^2)\delta\lambda = 0 \tag{34}$$

Equation (31) was included for completeness. Note that now there are four unknown functions of r and t, $\delta\lambda$, $\delta\nu$, $\delta\phi_1$ and $\delta\dot{\phi}_2$. There must be four independent equations. As with the equilibrium case, one is free to choose a set of four independent equations out of the five equations written above. One may choose, for example, equation (31) or equation (34) together with equations (27), (29) and (33) as the independent set. As before, I will choose equations (27), (29), (33) and (34). There is, however, an important point that was absent in the equilibrium case. Now, the continuity equation (equation (15) or, equivalently, equation (12) or equation (14) written for $\phi_2 = \phi_0\delta\dot{\phi}_2$) is not trivially satisfied but, instead, gives

$$\delta\dot{\phi}_2'' + \left(\frac{2}{r} + \frac{\nu_0' - \lambda_0'}{2} + 2\frac{\phi_0'}{\phi_0}\right)\delta\dot{\phi}_2' - \frac{1}{2}e^{\lambda_0-\nu_0}\omega(\delta\dot{\nu} - \delta\dot{\lambda}) - e^{\lambda_0-\nu_0}(\delta\dddot{\phi}_2 - 2\omega\delta\dot{\phi}_1) = 0 \ . \tag{35}$$

Note that this equation can not only be trivially integrated in time (justifying the ansatz $\phi_2 = \phi_0\delta\dot{\phi}_2$) but also with respect to the radial coordinate giving,

$$[r^2 e^{\frac{1}{2}(\nu_0-\lambda_0)}\phi_0^2\delta\phi_2']' + r^2\phi_0^2 e^{\frac{1}{2}(\lambda_0-\nu_0)}\omega[2\delta\phi_1 + \frac{1}{2}(\delta\lambda - \delta\nu) - \frac{1}{\omega}\delta\ddot{\phi}_2] = 0 \quad . \tag{36}$$

Thus, the set of equations obtained earlier is subject to the above constraint equation; not all solutions are allowed, but only those compatible with (36). Of course, the constraint equation is nothing else than the restriction that the radial perturbations should conserve the total number of particles. In fact, from the definition of N in equation (17), one obtains in first order in the perturbations,

$$\delta N = 8\pi\omega\int_0^\infty dr r^2 e^{\frac{1}{2}(\lambda_0-\nu_0)}\phi_0^2[2\delta\phi_1 + \frac{1}{2}(\delta\lambda - \delta\nu) - \frac{1}{\omega}\delta\ddot{\phi}_2] \quad . \tag{37}$$

Substitution of (36) into (37) gives immediately

$$\delta N = -8\pi\omega r^2 e^{\frac{1}{2}(\nu_0-\lambda_0)}\phi_0^2\delta\phi_2'|_0^\infty \quad . \tag{38}$$

In order to have $\delta N = 0$ (conservation of charge) the function $\delta\phi_2$ must have the appropriate radial behaviour at the boundaries. This restriction on $\delta\phi_2$ will later be translated into the choice of possible trial functions used to evaluate the eigenfrequencies of the perturbations. With this in mind, we can now go back to the independent set of equations, equations (27), (29), (33) and (34). From now on, it will prove convenient to introduce the notation $f_1(r,t) = \delta\phi_1(r,t)$ and $f_2(r,t) = \delta\phi_2'(r,t)$. The latter choice should be obvious from equations (33) and (38).

It is still not very clear how to extract the dynamics of the perturbations from the equations above. I will proceed by showing that it is possible to reduce the system to only two coupled equations for the real components of the perturbations on the scalar field. Note that in the case of fluid stars [7,8], the velocity of the perturbations can be related to a *single* "Lagrangian displacement", thus yielding only one final equation that governs the dynamics of the perturbations. Here, as we are dealing with a complex scalar field, we will naturally have two equations, rendering the problem of obtaining a variational principle more subtle.

Instead of taking equations (27) and (29) independently, it proves more convenient to take as independent equations, equation (27) and the combination (29)-(27),

$$\delta\nu' - \delta\lambda' = (\nu_0' - \lambda_0' + \frac{2}{r})\delta\lambda - 32\pi G r e^{\lambda_0}(m^2 + \frac{\lambda}{2}\phi_0^2)\phi_0^2 f_1 \quad . \tag{39}$$

Also, equation (33) can be trivially integrated in time giving,

$$\delta\lambda = 16\pi G r\phi_0(\phi_0' f_1 - \omega\phi_0 f_2) \quad . \tag{40}$$

The procedure now is tedious but simple. Using equation (40), it is possible to eliminate $\delta\lambda$ from the remaining equations, (27), (34) and (39). We can then differentiate equation (27) with respect to r and equate it to equation (39), eliminating $\delta\nu'$. The final result is a second order differential equation for the function $f_2(r,t)$,

$$\begin{aligned}
&f_2'' + 2\left(\frac{1}{r} + \frac{\phi_0'}{\phi_0} + \frac{3}{4}(\nu_0' - \lambda_0')\right) f_2' - e^{\lambda_0-\nu_0}\ddot{f}_2 + 2e^{\lambda_0-\nu_0}\omega \dot{f}_1' \\
&+ \Big[2(\nu_0' - \lambda_0')\left(\frac{1}{r} + \frac{\phi_0'}{\phi_0} + \frac{\nu_0' - \lambda_0'}{4}\right) - \frac{2}{r^2} + 2\frac{\phi_0''}{\phi_0} - 2\frac{\phi_0'^2}{\phi_0^2} + \frac{\nu_0'' - \lambda_0''}{2} \\
&+ 8\pi G r e^{\lambda_0-\nu_0}\omega^2\phi_0^2(\nu_0' - \lambda_0' + \frac{2}{r})\Big] f_2 \\
&- 8\pi G r e^{\lambda_0-\nu_0}\omega\phi_0\left((\nu_0' - \lambda_0' + \frac{2}{r})\phi_0' - 2e^{\lambda_0}(m^2 + \frac{\lambda}{2}\phi_0^2)\phi_0\right) \dot{f}_1 = 0.
\end{aligned} \tag{41}$$

Of course, the same dynamical equation would have been obtained had we used equation (31) instead. This is, in fact, a good consistency check. In order to obtain the analogous equation for $f_1(r,t)$, substitute $\delta\nu$ and $\delta\lambda$ as obtained respectively from equations (27) and (40) into equation (34). The resulting equation is,

$$\begin{aligned}
&f_1'' + \left(\frac{2}{r} + \frac{\nu_0' - \lambda_0'}{2} + 2\frac{\phi_0'}{\phi_0}\right) f_1' - 2\omega \dot{f}_2' - e^{\lambda_0-\nu_0}\ddot{f}_1 \\
&- \left[e^{\lambda_0}(4e^{-\nu_0}\omega^2 + \lambda\phi_0^2) + 16\pi G r\phi_0'\left(\frac{1}{r}\phi_0' + \phi_0'' + e^{\lambda_0}(e^{-\nu_0}\omega_0^2 + m^2 + \frac{\lambda}{2}\phi_0^2)\phi_0\right)\right] f_1 \\
&- \omega\left[\nu_0' - \lambda_0' + \frac{4}{r} + 4\frac{\phi_0'}{\phi_0} - 16\pi G r\phi_0(\frac{1}{r}\phi_0' + \phi_0'' + e^{\lambda_0-\nu_0}\omega^2\phi_0)\right] f_2 = 0 \quad .
\end{aligned} \tag{42}$$

The construction of a variational base closely follows that of Chandrasekhar [8]. Assume that all perturbations have a harmonic dependence on time of the form, $e^{i\sigma t}$, with σ being the characteristic frequency to be determined. We also let f_1 and f_2 stand for the amplitudes of the perturbations. It is then clear that equations (41) and (42) become eigenvalue equations for $f_2(r)$ and $f_1(r)$ respectively, with eigenvalue σ^2. They are, following Chandrasekhar's nomenclature [8], the "pulsation equations" of the problem. We must look for solutions to these equations satisfying the boundary conditions,

$$f_1(0) = f_2(0) = 0 \text{ and } \delta p_r \to 0 \text{ as } r \to \infty \quad , \tag{43}$$

where δp_r is defined in equation (30).

Inspection into equation (38) shows how the behaviour of f_2 at the origin is related to charge conservation. The requirement that both functions vanish at the origin insures that the perturbations have zero velocity at that point. The choice of boundary condition at infinity resembles, as closely as possible, the usual boundary condition for fluid stars $\delta p(R) = 0$. Writing it in terms of δp_r makes it independent of the choice of parametrization for the perturbations in equation (26). Also, it is compatible with the equilibrium results found for anisotropic spheres in the literature [9].

The system of coupled equations (41) and (42), together with the harmonic time dependence and the boundary conditions (43) constitute a characteristic value problem for σ^2. It can be shown that the problem is self-adjoint and that we can build a variational base to determine σ^2 if we multiply equations (41) and (42) by $G_2(r) = r^2\phi_0^2 e^{\frac{3}{2}(\nu_0-\lambda_0)}$ and $G_1(r) = r^2\phi_0^2 e^{\frac{1}{2}(\nu_0-\lambda_0)}$ respectively. The action integral that gives rise to the pulsation equations is then,

$$\begin{aligned}\sigma^2 \int_0^\infty [\frac{1}{2}e^{(\lambda_0-\nu_0)}(G_1 f_1^2 + G_2 f_2^2)]dr = \int_0^\infty &[\frac{1}{2}G_1 f_1'^2 + \frac{1}{2}G_2 f_2'^2 \\ &+ \frac{1}{2}G_1 C(r) f_1^2 - \frac{1}{2}G_2 H(r) f_2^2 - \omega G_1 f_2(2f_1' + f_1 L(r))]\, dr \quad ,\end{aligned} \tag{44}$$

where we have introduced

$$\begin{aligned}C(r) \equiv& e^{\lambda_0}(4e^{-\nu_0}\omega^2 + \lambda\phi_0^2) \\ &+ 16\pi G r\phi_0'[\frac{1}{r}\phi_0' + \phi_0'' + e^{\lambda_0}(e^{-\nu_0}\omega^2 + m^2 + \frac{\lambda}{2}\phi_0^2)\phi_0]\end{aligned} \tag{45}$$

$$\begin{aligned}H(r) \equiv& 2(\nu_0' - \lambda_0')(\frac{1}{r} + \frac{\phi_0'}{\phi_0} + \frac{\nu_0' - \lambda_0'}{4}) - \frac{2}{r^2} + 2\frac{\phi_0''}{\phi_0} - 2\frac{\phi_0'^2}{\phi_0^2} + \frac{\nu_0'' - \lambda_0''}{2} \\ &+ 8\pi G r e^{(\lambda_0-\nu_0)}\omega^2\phi_0^2(\nu_0' - \lambda_0' + \frac{2}{r})\end{aligned} \tag{46}$$

and

$$L(r) \equiv 16\pi G r\phi_0\left(\frac{1}{r}\phi_0' + \phi_0'' + e^{(\lambda_0-\nu_0)}\omega^2\phi_0\right) \quad . \tag{47}$$

Note that the orthogonality condition related to different characteristic values of σ^2 is given by

$$\int_0^\infty \frac{1}{2}e^{(\lambda_0-\nu_0)}(G_1 f_1^i f_1^j + G_2 f_2^i f_2^j)dr = 0 \quad (i \neq j), \tag{48}$$

where the (i,j) indices represent the solutions for different characteristic values of σ^2 .

In the spirit of Chandrasekhar's work [8], we can state that since equation (44) expresses a minimal principle, *a sufficient condition for the dynamical instability of a bosonic stellar configuration with the interactions defined in (1) is that the right hand side of equation (44) vanishes for some given trial functions f_1 and f_2 satisfying the boundary conditions (43).* In the next section the above formalism will be applied to the particular cases $\Lambda = 0$ and $\Lambda = 60$. (Remember that in section 2 we introduced $\Lambda = \frac{\lambda M^2_{Planck}}{8\pi m^2}$).

5. Looking for Instabilities

The first step in finding dynamical instability is to numerically solve the equilibrium equations (18)-(20), since all coefficients in (44) depend on the equilibrium solutions. I refer the reader to references [2,5] for details. For us it is important to stress the fact that each equilibrium configuration is parametrized by a given value of the central density, which is used as an initial condition on the integration of equations (18)-(20). Once we have the equilibrium configurations, we can evaluate numerically the integrals in (44) for a given pair of trial functions obeying the boundary conditions (43), with different values of the central density. Dynamical instability will be present whenever the right hand side of (44) is less than or equal to zero.

In order to look for instabilities we can concentrate just on the right hand side of equation (44); the coefficient multiplying σ^2 on the left hand side is positive definite and will only "normalise" the value of the eigenfrequencies. It then proves useful to write the integral (call it I) on the right hand side of (44) as

$$I = x^2 C_1 + C_2 + xC_3 \quad , \tag{49}$$

where

$$C_1 \equiv \int \frac{1}{2} G_1 [f_1'^2 + C(r) f_1^2] \tag{50}$$

$$C_2 \equiv \int \frac{1}{2} G_2 [f_2'^2 - H(r) f_2^2] \tag{51}$$

$$C_3 \equiv \int \omega G_1 f_2 [2f_1' + f_1 L(r)] \tag{52}$$

and $x \equiv a/b$ comes from multiplying the trial functions f_1 and f_2 by the arbitrary numbers a and b respectively (there is always freedom in the choice of multiplicative coefficients for the trial functions) and by dividing equation (44) by b^2. Thus, if $I \leq 0$ for a given pair of trial functions we have found dynamical instability. In fact it can be stated that a sufficient condition for dynamical instability is that

$$C_3^2 - 4C_1 C_2 \geq 0 \quad . \tag{53}$$

Clearly, once this condition is satisfied, one can always find two (or one if (53) is an identity) real numbers $x_{1,2}$ just by solving the algebraic equation obtained by equating (49) to zero. As $C_1 > 0$ for all ranges of interest (the function $C(r)$ defined in (45) is positive definite for $0 < \sigma(0) < 2.0$), we can make $I \leq 0$ just by picking the ratio a/b within the limits $x_1 \leq a/b \leq x_2$. Thus, to look for instabilities just pick a pair of trial functions f_1 and f_2 that obey the boundary conditions (43) and the constraint of charge conservation and evaluate the integrals C_1, C_2 and C_3 defined in equations (50)-(52). Check if the condition (53) is satisfied. If it is, the system is unstable for that central density and for that pair of trial functions. It is then a cosmetic matter to explicitly evaluate the eigenvalue by obtaining $x_{1,2}$ from (49) and using the information in equation (44).

As trial functions are used as approximations to the real solutions to evaluate (44), it is only possible to put an upper bound on the value of the central density where dynamical instability intervenes, $\sigma_{ins}(0)$. In choosing possible trial functions, I have used the well known ansatze of the stability analysis of fluid stars [7,8] compatible with the requirement of charge conservation. After a thorough (but not exaustive) search, I found that the smaller values for $\sigma_{ins}(0)$ were obtained, independently of Λ, for the pair

$$f_1 = xe^{\nu_0/2} \quad ; \quad f_2 = x\phi_0 \quad , \tag{54}$$

where the multiplicative constants a and b were left out. They can be easily evaluated for each particular case.

The ansatz for f_1 is, in fact, the same used by Chandrasekhar in his stability analysis of homogeneous spheres with constant energy density [8]. In figures 1 and 2 the upper bounds for the occurence of dynamical instability are shown for $\Lambda = 0$ and $\Lambda = 60$, respectively, in a plot of total mass against $\sigma(0)$. The upper values of $\sigma_{ins}(0)$, $\sigma_{ins}(0) \geq 0.98$ and $\sigma_{ins}(0) \geq 0.45$ are indicated by dots. Note that the instabilities occur well after the maximum mass.

Although it is possible, in principle, to find "better" upper values for $\sigma_{ins}(0)^\dagger$, the fact is that the results are quite different from those for fluid stars. The instabilities seem to occur well after the critical point, even after the crossing point where $E_b = 0$. These results can certainly be linked to the fractional anisotropy characteristic of these objects. The fractional anisotropy being positive definite seem to provide extra support against small perturbations. From table 1 and figures 3 and 4, it is easy to see that a bigger value for Λ has the consequence of decreasing the FAR. Table 3 offers yet another way of confirming this result, by listing the values of $\sigma_{ins}(0)$ and $\sigma_{crit}(0)$ for different values of Λ. Notice that both quantities decrease with growing Λ, although the change is not monotonic. Clearly, in the isotropic case, the two values for $\sigma(0)$ such be identical.

† For example, the inequality (53) can be trivially satisfied if $C_2 < 0$. By studying the behaviour of the function $H(r)$ defined in (46), it is possible to choose trial functions that will make $C_2 < 0$. In practice, though, this task is not so simple [10].

6. Closing Remarks

A variational formalism, in the framework of general relativity, was developed to examine the occurence of dynamical instability against small, radial perturbations on bosonic stellar configurations obtained from massive, self-interacting (with $V(\phi) = \frac{\lambda}{4}|\phi|^4$) complex scalar fields.

Adapting Chandrasekhar's formalism to a microscopic context, it was possible to find an upper bound for the value of the central density where dynamical instability intervenes both for the free case and for the repulsive, self-interactive case. The results indicate that the instabilities occur to the right of the maximum in the curve of mass against central density of the equilibrium configurations (figures 1 and 2 and table 3), contrary to the conjecture [3-5] that they should occur at the maximum. Nevertheless, it should be stressed that this conjecture is based on theorems applicable only for fluid stars with an isotropic equation of state. As explained in sections 2 and 3, local anisotropy certainly plays an important role in determining the structure of boson stars. In particular, as shown in section 5, it is intrinsically related to the stability properties of the equilibrium configurations. The present results are corroborated by the analysis of Colpi, Shapiro and Wasserman for the large coupling limit [5], where it is possible to approximately describe the configuration with an effective isotropic equation of state; the larger the coupling the smaller the fractional anisotropy and the better the approximation of an isotropic perfect fluid.

Of course, the possibility that better trial functions can decrease the upper bounds found in the present work for dynamical instability is not totally excluded. However, based on preliminary calculations, it seems very difficult to improve the bounds so dramatically as to have the instabilities at the maximum value for the mass.

Certainly, the study of anisotropic compact objects promises to be a very interesting field of investigation. It should be possible to generalize the present approach to any anisotropic object either by formulating the problem from a field theoretical point of view or by adapting the perfect fluid analysis to the anisotropic case [10]. In the latter case one would need 2 equations of state in order to establish the variational formalism. What would be the relationship between the tangential pressure and the energy density? Also, the dynamics of the gravitational collapse of these objects, together with the possible formation of scalar black holes (the particle number would probably be one of the charges of the scalar black hole) and its connection with thermodynamics (is the loss of quantum numbers translated into the black hole's entropy ?) deserve further study.

Acknowledgments

I would like to thank Professor S. Chandrasekhar for a very useful conversation and for his interest in the project. I also would like to thank E. Copeland, K. Lee, M. Mangano and J. Stein-Schabes for their constant interest and support. Finally, I thank P. Jetzer for many important discussions.

Figure Captions

Figure 1. Boson-star mass in units of M^2_{Planck}/m (continuous line) and particle number in units of M^2_{Planck}/m^2 (dotted line) as a function of the central density for $\Lambda = 0$. The dot represents the upper value for stability.
Figure 2. Boson-star mass in units of M^2_{Planck}/m (continuous line) and particle number in units of M^2_{Planck}/m^2 (dotted line) as a function of the central density for $\Lambda = 60$. The dot represents the upper value for stability.
Figure 3. The fractional anisotropy as a function of the radial coordinate for $\Lambda = 0$ for 3 different equilibrium configurations. The dots represent the value of the fractional anisotropy at the radius of the configurations. The straight line is a good fit to within a few percent.
Figure 4. The fractional anisotropy as a function of the radial coordinate for $\Lambda = 60$ for 3 different equilibrium configurations. The dots represent the value of the fractional anisotropy at the radius of the configurations. The straight line is a good fit for central values of $\sigma(0)$.

Table Captions

Table 1. The value of the fractional anisotropy at the radius for different values of the central density and for different values of Λ. Note how the FAR drops for bigger values of Λ.
Table 2. The ratio between the values of the central density at the maximum $\sigma_{crit}(0)$ and at the crossing point $\sigma_{crs}(0)$ for different values of Λ.
Table 3. Values of the central density at the maximum $\sigma_{crit}(0)$ and at the upper value for stability $\sigma_{ins}(0)$ for different values of Λ.

References

[1] R. Friedberg, T. D. Lee and A. Sirlin, *Phys. Rev.* **D13** (1976)2739; S.Coleman, *Nucl. Phys.* **B262** (1985)263. For a recent work on the possible cosmological relevance of these objects see, J. Frieman, G. Gelmini, M. Gleiser and E. Kolb, *Solitogenesis: Primordial formation of non-topological solitons*, Fermilab report Pub-88/13-A (1988), to appear in Phys. Rev. Lett.

[2] R. Ruffini and S. Bonazzola, *Phys. Rev.* **187** (1969)1767.

[3] E. Takasugi and M. Yoshimura, *Z. Phys.* **C26** (1984)241; J. D. Breit, S. Gupta and A. Zaks, *Phys. Lett.* **140B** (1984)329; T. D. Lee, *Phys. Rev.* **D35** (1987)3637; R. Friedberg, T. D. Lee and Y. Pang, *Phys. Rev.* **D35** (1987)3640.

[4] J. J. van der Bij and M. Gleiser, *Phys. Lett.* **194B** (1987)482.

[5] M. Colpi, S. L. Shapiro and I. Wasserman, *Phys. Rev. Lett.* **57**(1986)2485.

[6] R. Friedberg, T. D. Lee and Y. Pang, *Phys. Rev.* **D35** (1987)3658; T. D. Lee and Y. Pang, *Phys. Rev.* **D35** (1987)3678.

[7] There are many text books where the problem of dynamical instability of fluid stars is discussed. See, for example, S. L. Shapiro and S. A. Teukolsky, 'Black Holes, White Dwarfs and Neutron Stars, the Physics of Compact Objects', (J. Wyley and Sons, New York, 1983). See also, Ya. B. Zel'dovich and I. D. Novikov, 'Relativistic Astrophysics' vol. 1, (The University of Chicago Press, Chicago, 1971).

[8] S. Chandrasekhar, *Phys. Rev. Lett.* **12** (1964)437, *Ap. J.* **140** (1964)417.

[9] R. L. Bowers and E. P. T. Liang, *Ap. J.* **188** (1974) 657.

[10] M. Gleiser, *Anisotropic Compact Objects*, work in progress.

$\sigma_0(0)$	fa_0	$\sigma_{60}(0)$	fa_{60}	$\sigma_{200}(0)$	fa_{200}
0.1	1.085	0.1	0.353	0.05	0.137
0.271	1.088	0.16	0.241	0.094	0.066
0.54	1.105	0.327	0.245	0.195	0.078
1.02	1.208	0.7	0.384	0.3	0.118

Table 1

Λ	$\sigma_{crit}(0)$	$\sigma_{crs}(0)$	$\sigma_{crs}(0)/\sigma_{crit}(0)$
0	0.271	0.54	1.99
60	0.158	0.312	1.97
200	0.094	0.195	2.1

Table 2

Λ	$\sigma_{crit}(0)$	$\sigma_{ins}(0)$
0	0.271	0.98
60	0.158	0.45
200	0.094	0.32

Table 3

Figure 1

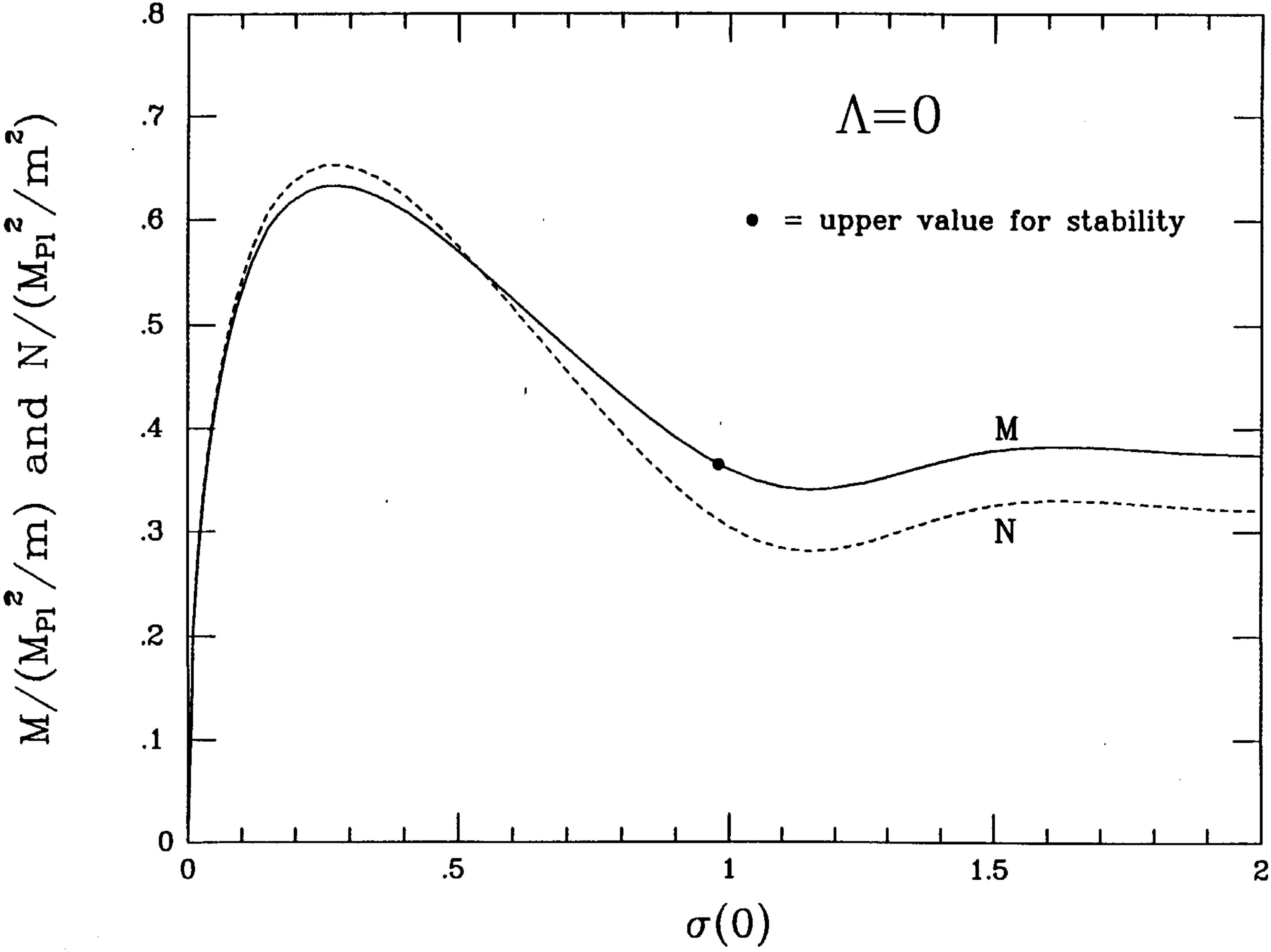

$\Lambda=0$
● = upper value for stability
M
N
$M/(M_{Pl}^2/m)$ and $N/(M_{Pl}^2/m^2)$
$\sigma(0)$
0
.1
.2
.3
.4
.5
.6
.7
.8
0
.5
1
1.5
2

Figure 2

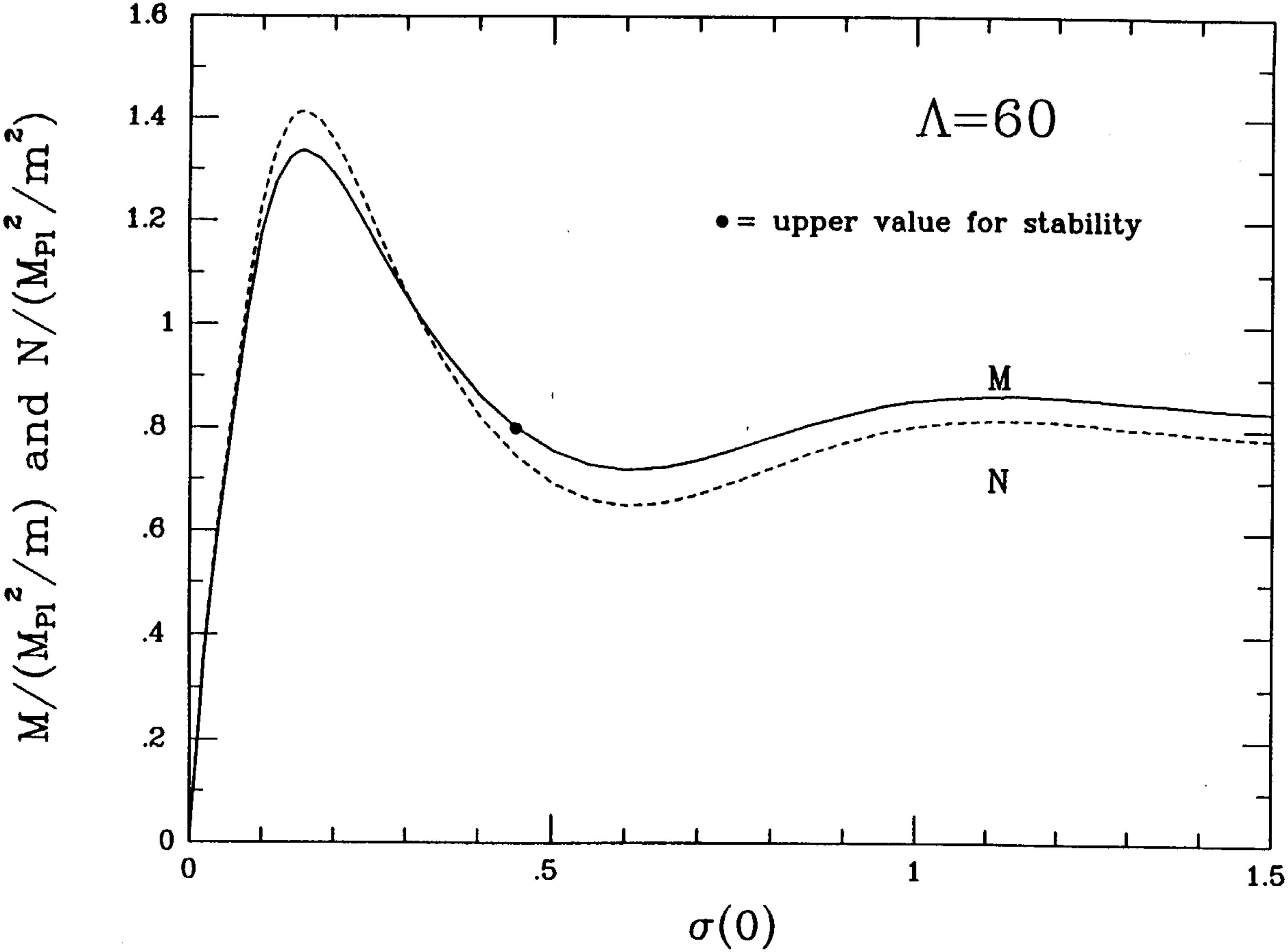

Λ=60
● = upper value for stability
M
N
1.6
1.4
1.2
1
.8
.6
.4
.2
0
0
.5
1
1.5
$M/(M_{Pl}^2/m)$ and $N/(M_{Pl}^2/m^2)$
$\sigma(0)$

Figure 3

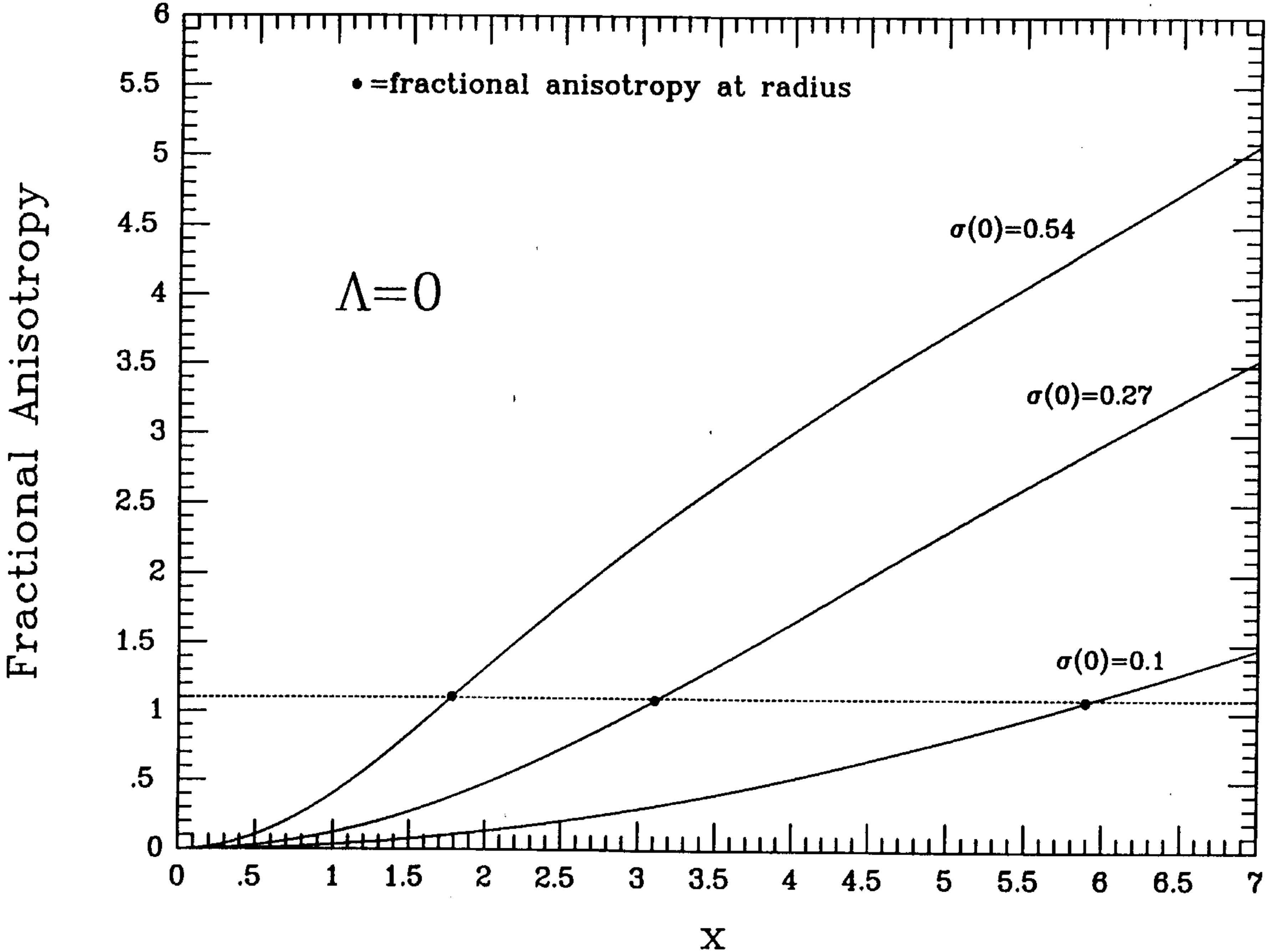

• =fractional anisotropy at radius
Λ=0
σ(0)=0.54
σ(0)=0.27
σ(0)=0.1
Fractional Anisotropy
X
0
.5
1
1.5
2
2.5
3
3.5
4
4.5
5
5.5
6
6.5
7

Figure 4

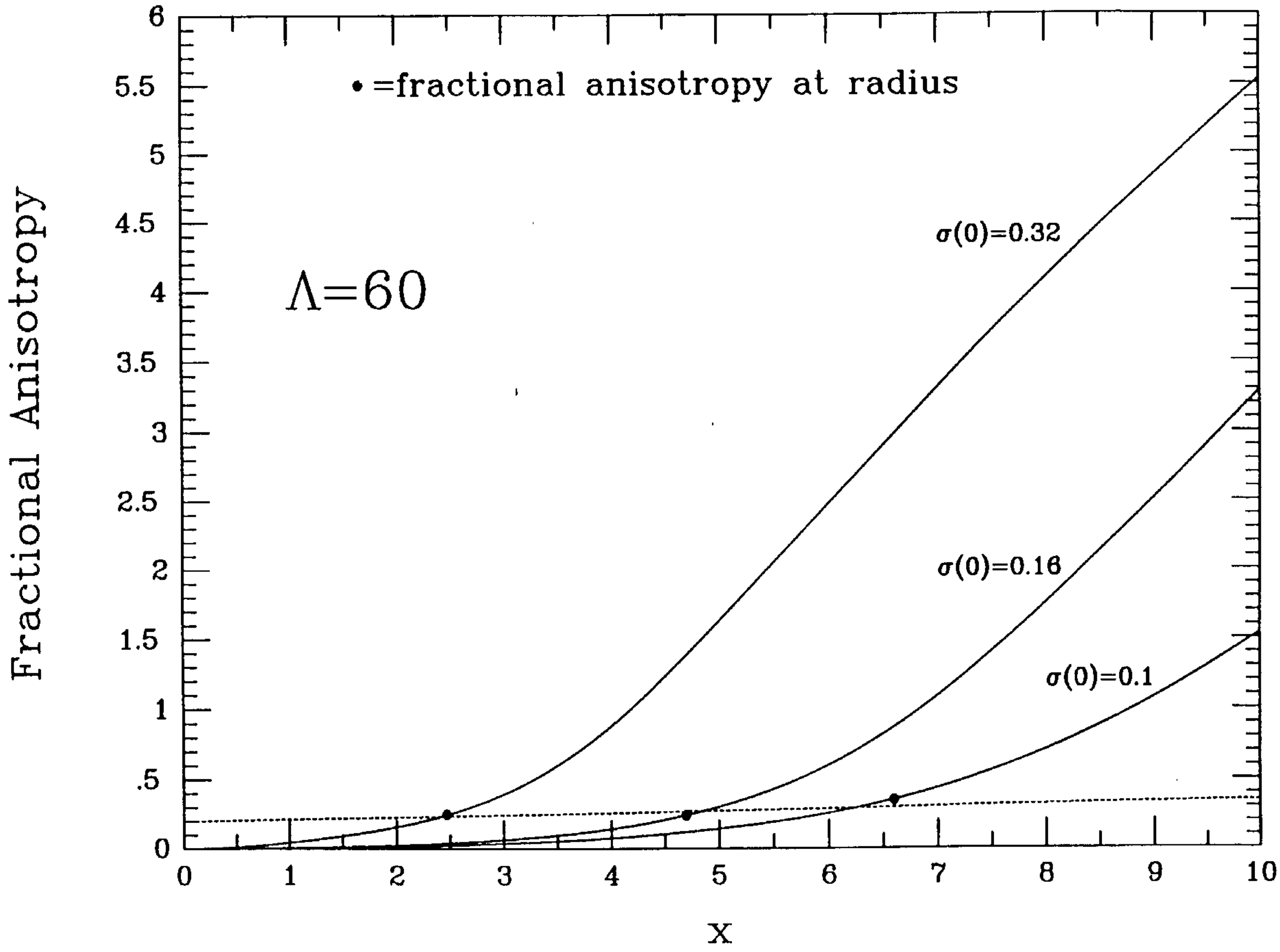

• =fractional anisotropy at radius
Λ=60
σ(0)=0.32
σ(0)=0.16
σ(0)=0.1
Fractional Anisotropy
X
0
.5
1
1.5
2
2.5
3
3.5
4
4.5
5
5.5
6
0
1
2
3
4
5
6
7
8
9
10